Egypt. J. Chem. **Vol. 66**, No. SI: 13 pp. 1719 - 1732 (2023)

Egyptian Journal of Chemistry

http://ejchem.journals.ekb.eg/

Attenuation Roles of Bioactive Compounds from Grapefruit against Silver Nanoparticles Induced Pulmonary Toxicity and Oxidative Stress

Eman A. Younis, Hanan F. Aly, Sanaa A. Ali*

Department of Therapeutic Chemistry, National Research Centre, El-Buhouth St. Postal Code 12622, Dokki, Giza, Egypt

Abstract

The therapeutic potential of methanolic extract, pectin, hesperidin, and naringin derived from *Citrus paradisi* peel (grapefruit) was investigated against the toxicity of silver nanoparticles (AgNPs). Mice received orally AgNPs of size 20 &100nm for four weeks then treated with methanolic extract, pectin, hesperidin, and naringin for three weeks. *C. paradisi* peel yielded methanolic extract (11.37%), pectin (30.88%), naringin (4.3%) and hesperidin (0.09%),the results showed a significant reduction in lung tissue ; Adenosine triphosphate ,Adenosine diphosphate and Adenosine monophosphate respectively (ATP, ADP, AMP) , total adenylate (TA), inorganic phosphate (IP), phosphate potential (PP), and adenylate Energy Charge (AEC). Besides, obvious decrease in both vitamin E and C levels in both sizes of Ag–intoxicated, along with marked inhibition in superoxide dismutase (SOD) and catalase antioxidant enzyme activities. While oxidative stress marker, MDA was significantly elevated. More severe damage was detected with a smaller size of 20 nm than 100 nm AgNP particle size compared to the control mice. Histopathological examination revealed inflammation and cellular degeneration caused by AgNPs after, treatment with the above compounds showing repair ease. *C. paradisi* derived by products including phenolic extract, pectin, hesperidin, and naringin that are handled unexpectedly as promising competitor remedial specialists against poisonousness induced by AgNPs in mice.

Keywords: *Citrus paradisi* , Silver nanoparticles; ATP; ADP; AMP; AEC; Particle sizes; *Citrus paradisi*; Phenolic compounds; Pectin; Hesperidin; Naringin

1. Introduction

The quickly meddling field of nanotechnology has offered innovative disclosures in clinical, mechanical, and purchaser territories. One of the kind physicochemical and electrical properties of the planned nanoparticles makes them significantly charming in a combination of applications, variations in basic and physicochemical properties of nanoparticles can prompt contrasts in organic exercises including ROS creations, one of the most possible revealed NP associated poison levels [1]. The use of AgNPs in purchaser passages is regularly expanding because of the high anti-infection movement of silver, the amassing AgNPs is important to check bacterial and parasitic tainting of materials, food bundling, beautifying agents, inserts, or other clinical specialties [2]. AgNPs gain entry into the body of an animal through oral ingestion, actual contact (through skin sores or scraped areas), aspiratory inward breath, and intravenous/intraperitoneal injection for either therapeutic purposes or diagnostic [3]. Oxidative stress-induced by designed NP is because of cell substitutions, for example, molecule surface, size, structure, and presence of metals, while cell activities, for example, mitochondrial breath, NP cell association, and safe cell enactment, are liable for ROS-mediated scratch [4]. Oxidative stress is a critical determinant of NP-instigated injury; it is a major choose the ROS reaction going to NP, beyond the physicochemical indicators and consciousness of the different flagging falls run by NP-prompted ROS [5].

The inflammatory, DNA-harming, and cytokine-inductive properties of AgNPs are well known

*Corresponding author e-mail: Sanaa _ahmedibrahim@yahoo.com.; (Prof.: Sanaa Ahmed Ali).

EJCHEM use only: Received date 17 July 2023; revised date 07 August 2023; accepted date 16 August 2023

DOI: 10.21608/EJCHEM.2023.223508.8270

[6].The safety parts of Ag-NP have focused on the effects of Ag-NP helper to an oral, intravenous, or intraperitoneal application [7]. In the lung AgNPs show a high inflammatory potential, granulomatous injury, concerning the biokinetic properties of AgNPs, it shows sensible to expect that little AgNPs allow the epithelial lung boundary and travel to far off organs through the blood and additionally the lymphatic fluid [8].

Citrus peels as a source of antioxidant constituents; they contained a diversity of polyphenols with the highest concentration than pulp and juice, which illustrated the highest antioxidant capacity [9]. Citrus fruits are expended around the world, yielding a major quantity of citrus peels. Among citrus fruits, grapefruit (*Citrus paradisi*) originated from interspecific hybridization between pummeling (*Citrus maxima*) and sweet orange (*Citrus sinensis*) [10]. Recently, *C. paradisi* has attracted much awareness because of its assumed medicinal properties such as antioxidant, antimicrobial, anticancer, ant-proliferative, and anti-inflammatory activities as well as cardiovascular and anti-hypertensive properties [11]. Grapefruit peel offers various promising bioactive compounds beyond volatile and nonvolatile phytochemical such as terpenes, flavonoids, carotenoids, limonoids, organic acids, pectin, and folate [12,13]. Furthermore, *C. paradisi* contained essential and volatile oils composed mainly of limonene alongside other bioactive compounds including, monoterpenes, monoterpene oxide, sesquiterpene, and sesquiterpene oxide. They diffuse the growth and proliferation of neuroblastomas, leukemias, prostate, and lung cancer lines [14]. Naringin was the dominant flavonoid compound in the peel of grapefruit [9]. Another reasonable product that can be obtained from *C. paradisi* fruit peels is pectin**,** which has showy immunoregulatory, anti-inflammatory, hypoglycemic, antibacterial, antioxidant, and antitumor activities [15].

In this routine diagnosis, we illustrate the effect of AgNPs with small and large particle sizes associated with oxidative damage-induced lung toxicity. It can be achieved through the determination of ATP, ADP, AMP, TA, IP, PP, vitamins E and C antioxidant enzymes; catalase, oxidative damage; MDA. Besides, the advanced effects and chemical characterization of methanolic extract, pectin, hesperidin, and naringin isolated from *C. paradisi* fruit peels will be elucidated.

2. Materials and methods

2.1. Plant materials

2.1.1. Chemicals

Silver nanoparticles (20 nm and 100 nm) were surrendered by Sigma-Aldrich CO. (St Louis, Missouri, USA). Biochemical boundaries were shown using Biodiagnostic Kits (Biodiagnostic Co., Egypt)

All chemicals and HPLC principles used were of high systematic evaluation. Hesperidin (≥80%, Sigma Aldrich, Spain), Naringin (≥95%, Sigma Aldrich, United Kingdom), and Naringenin (≥95%, Sigma Aldrich, Germany) were purchased. Other phenolic and flavonoid standards such as pyrogallol, gallic acid, *p*-hydroxybenzoic acid, *p*-coumaric acid, ferulic acid, caffeic acid, vanillic acid, gantisic acid, cinnamic acid, syringic acid, and sinapinic acids. Flavanol: Catachin; flavonol: quercetin, kaempferol, myricetin; flavonol glycoside: rutin. Flavone: Apigenin, apigenin-7-glucoside was purchased from Sigma-Aldrich Co. USA.

2.1.2. General procedure

Agilent Technologies 1100 arrangement fluid chromatography furnished with an autosampler and a diode-cluster locator (DAD) HPLC assessment [16]. The diagnostic section was an Eclipse XDB-C18 (150 x 4.6 µm; 5 µm) with a C18 monitor segment (Phenomenex, Torrance, CA). The portable stage is comprised of acetonitrile and acidic corrosive 2% in water (v/v) (solvent A and B) respectively. The slope was modified as follows: 0-5 min, 100% B (isocratic step); 30 min, 100-85% B (direct inclination); 20 min, 85-half B (straight angle); 5 min, 50-0% B (straight angle); 5 min, 0 - 100% B (straight angle) at a stream pace of 0.8 ml min-1. 20 µl was infused; tops were checked all the while at 280, 320, and 360 nm for the benzoic corrosive, cinnamic corrosive subordinates, and flavonoid, respectively.0.45 µm Acrodisc needle channel (Gelman Laboratory, MI). Harmonious maintenance times and UV spectra are known by tops and contrasted and those of the norms.

Proton Nuclear Magnetic Resonance (^{1}HNMR) experiments were designed on JEOL EX-500 spectroscopy (Tokyo, Japan) (400 MHz) handling DMSO-d_6 as the solvent and internal specifies.

2.1.3. Plant materials

The fresh fruit of *C. paradisi* (pink grapefruit) was purchased in January 2017 from NRC Farm, Giza, Egypt. The fruits were washed; the peels

including flavedo and albedo were peeled off and then minced.

2.1.4. Polyphenolic compounds extraction

Initially, the minced fresh peel of *Citrus paradisi* was extracted with petroleum ether at 40-60ºC. Dried defatted marc was soaked in absolute methanol at room temperature. The extraction refined was repeated tribulations and, the filtrate was consolidated and afterward was vanished under vacuum in revolving evaporator at 40 ºC yielded, crude extract, weighted and subjected to HPLC/DAD analysis.

2.1.5. Isolation of Pectin

The dried marc left after extraction of methanol extract was downed in distilled water at a solid to dissolvable proportion of 1:15 (w/v). The combination was shaken on a shaker. Then, the combination was warmed at 80 °C for 2 h; the step was repeated double the time. The combination was cooled to room temperature then, filtrated through muslin and filter paper. The filtrate was concentrated on the rota-evaporator. Ethanol 95% (ratio 1: 2) was added to the concentrated syrup yielding mucilage/pectin (P1). The precipitate was washed with ethanol and acetone. Further, the marc remaining after hot extraction of mucilage/ pectin was heated with 0.3% ammonium oxalate solution (1:15) for one hour at 90°C and then filtered through muslin. It was repeated twice and the combined extract was cooled. Ethanol 95% was added to the aqueous extract in ratio the 1:2 stirring and allowed to stand for 30 min. to allow pectin (P2) to float on the tops when most of pectin free solvent could be removed by siphoning. The precipitate was pressed on a muslin bag and washed with the absolute ethanol and acetone. Then dried in freeze drier and subjected to physio-chemical characterization [16].

2.1.6. The molecular weight distribution of pectin (P2)

The peak molar masses were estimated by gel permeation chromatography (GPC) with the Agilent 1100 series (Germany) at room temperature using two columns, PL aqua gel-OH (7.5mm id, 30µm pore size, 8 µm particle size) and PL aqua gel-OH (7.5mm id, 50µm pore size, 8 µm particle size) using a refractive index detector, a flow of 1.0 mL min-1, 0.5% pectin concentration. 0.01 N NaN3 and water were used as running solvents and polyethylene oxide/ glycol were used as standard.

2.1.7. Fourier transforms Infra-Red analysis for pectin (P2)

The Fourier transform IR spectrum of the pectin (P2) was recorded in a frequency range of 400-4000 cm-1 using of KBr pellets on FT/IR-6100 (JASCO, Japan).

2.2. Biological study

2.2.1. Reagents

Biochemical boundaries were shown using Biodiagnostic Kits (Biodiagnostic Co., Egypt).

2.2.2. ***Homogenate of lung tissue***

Homogenization of lung tissue was conducted in 0.9 ml/L NaCl (1:10 w/v) for the evaluation of energetic parameters, oxidative stress, vitamin C, E and antioxidant enzymes; SOD and catalase [17].

2.2.3. ***Energetic parameter evaluation***

ATP was indexed [18]. ADP and AMP were scheduled in a single measure framework according to Jaworek et al. [19].

2.2.4. ***Phosphate potential Calculation (PP)***

It is an elective document used to outline the free energy status of the tissues and can be resolved from the focal point of ATP, ADP and Pi of ATP, ADP and Pi [20] PP = [ATP]/[ADP] [Pi].

2.2.5. ***Calculation of total adenylate***

TA = ATP + ADP + AMP.

2.2.6. ***Adenylate energy charge calculation***

AEC = 1/2 [ADP + ATP]/ [AMP + ADP + ATP].

2.2.7. ***Inorganic phosphates (IP)***

Inorganic phosphates were recorded in a similar concentrate in which ATP ADP and AMP were accounted for [21].

2.2.8. ***Estimation of malondialdehyde (MAD)***

It was conducted according to Buege and Aust [22].

2.2.9. ***Estimation of catalase enzyme activity***

It was produced by colorimetric assay [23].

2.2.10. ***Estimation of superoxide dismutase***

It brought about a colorimetric assay method according to Nishikimi et al.[24].

2.2.11. Folin reagent was used in the assurance of vitamin C

The confirmed shading was estimated at 560 nm [25]. Furthermore, nutrient E was evaluated by

utilizing a spectrophotometric technique by Das et al. [26].

2.3. Animals

The healthy Swiss Albino mice, weighting 25-35g, were obtained from the creature house, National Research Center of Egypt. The neighborhood panel affirmed the plan of the investigations, and the convention relates to the rules of the National Research Centre. Before, exploratory mice were adjusting multi-week under the research facility conditions. After the acclimation time frame, mice were housed in tempered steel confines feed on the standard pellet diet, and faucet water was not indispensable Animals.

2.4. Experimental design

Two hundred and twenty-five male mice (25-30 gm.) were divided into fifteen groups (15 mice each).

Group 1: Control group.

Groups 2&3: Induced toxicity of aggregates of small and large-sized 20 nm; 100 nm AgNPs (100 mg/kg) for one month [1]

Groups 4&5: Control given methanolic extract (500 mg/kg), pectin (200 mg/kg) [27].

Groups 6&7: +ve 20nm AgNPs treated with methanolic extract (500 mg/kg), pectin (200 mg/kg), respectively.

Groups 8&9:+ve 100 nm AgNPs treated with methanolic extract (500 mg/kg), pectin (200 mg/kg), respectively.

Groups 10&11: Control given hesperidin (100 mg/kg), naringin (100 mg/kg) [28, 29].

Groups 12&13: +ve 20nm AgNps treated with hesperidin (100 mg/kg), naringin (100 mg/kg), respectively.

Groups 14&15: +ve 100nm AgNPs treated with hesperidin (100 mg/kg), naringin (100 mg/kg), respectively.

2.5. Histopathological examinations

The lung was cut and soaked in a graded series of alcohol and fixed in paraffin wax. 5µm thick bits were cut and stained by hematoxylin and eosin (H&E), the research was done using a light microscope [30].

2.6. Statistical analysis

Information was examined with SPSS (Statistical Package for the Social Sciences) rendition 9.05 programming (USA). Information are introduced the mean ±SE. Critical contrasts between the gatherings were factually dissected by a single direction examination of change (ANOVA) Followed by Turkey's different correlations post hoc test, a measurable distinction of $P < 0.05$ was viewed as significant.

2.7. Ethical statement

All experiments were approved by the Animal Ethical Committee of the Medical Division, National Research Centre, so that animals did not suffer pain at any stage of the experiment (Ethical **Approval No: 11445062023).**

3. Results

3.1. Biochemical analysis

Table (1) showed an insignificant change in ATP, AMP, AMP, TA, IP, AEC, and PP levels upon treating normal mice with methanolic extract, pectin, hesperidin, and naringin.

Table (2) Exposure to 20nm Ag declared a severe significant reduction at the nucleotide level; ATP, ADP, and AMP, reached to 67.65, 50.00, and 53.85 %, respectively. Otherwise, the treatment of Ag–intoxicated mice with methanol extract, pectin, hesperidin and naringin exhibited marked improvement in ATP, ADP, and AMP, levels with the highest improvement percentages for ATP with hesperidin (57.35%), ADP with pectin (35.71%) and AMP with naringin (76.92%). Mice intoxicated with 100 nm size Ag declared a significant reduction (70.59%). Additionally, marked reduction in ADP and AMP levels with percentages of 60.71 and 69.23%, respectively. Noticeable amelioration in ATP, ADP, and AMP levels with the highest improvement percentages for hesperidin (45.59, 32.14, 100%), respectively for ATP, ADP, and AMP followed by pectin (41.18, 28.57, and 76.92%, respectively). A significant reduction in PI is recorded with a percentage of 47.46%. Also, a significant reduction in AEC, and PP in Ag–intoxicated mice (43.04 and 83.46%, respectively) was observed. A medication of intoxicated mice with crude methanol extract, pectin, hesperidin, and naringin exhibited noticeable improvement in all detected parameters with obvious ease with hesperidin, which recorded 94.92, 30.38, and 63.23%, respectively for IP, AEC, and PP, followed by pectin (91.53, 26.58, and 55.45%, respectively).

TA showed a marked reduction in both particle sizes (20 and 100 nm) and Ag recording 61.47 and 67.89%, respectively. Medication with hesperidin showed the highest improvement percentages in TA (54.13 and 48.62%, respectively) for the two sizes, followed by pectin, methanolic extract, and naringin.

Furthermore, however, a significant increase in IP with both 20 and 100 nm Ag reached 67.8% and

47.46% respectively. A high percent of enhanced with methanol extract, pectin, hesperidin, and naringin with 74.58, 81.36, 84.75, and 71,19 respectively in 20 nm and 86.44, 91.53, 94.92, and 79.66 respectively in 100 nm was observed. AEC and PP exhibited a significant reduction, recorded at 34.18 and 87.35%, respectively, in 20 nm. While 43.04 and 83.46, respectively in case 100 nm, after treatment of the 20 nm intoxicated mice with pectin and hesperidin showed the highest percentages of improvement 26.58 and 26.58%, respectively for AEC. PP recorded 86.58 and 98.25%, respectively, in 100 nm, 26.58 and 30.38% respectively. Catalase, SOD, MDA, Vitamin C and Vitamin E showed insignificant change upon treated normal mice with different materials, as revealed in Table (3).Obvious amelioration in Catalase, SOD, MDA, Vit. C and Vit.E were detected upon treated both silver sizes nanoparticles with methanolic extract and active components; pectin, hesperidin, and naringin showed the highest percentages of improvement for hesperidin followed by pectin, methanolic extract, and finally naringin as shown in Table (4).The histological score shown in Table (5) for the effects of bioactive compounds in lessening lung inflammation/injury

Concerning to phytochemical study of *C. paradisi* peel, the methanol crude extract yielded, 227.5g ± 1.87 (11.37% of fresh peel). The polyphenol composition of methanolic crude extract was qualitatively and quantitatively determined by HPLC/DAD comparing their retention time with available authentic as aforementioned and the results were recorded in Table (6). Seven phenolic compounds, including *p*-hydroxybenzoic, chlorogenic, caffeic, ferulic, cinnamic and *p*-coumaric acids also pyrogallol identified in the *C. paradisi* extract. Likewise, seven flavonoids; narirutin, naringin, hesperidin, apigenin-7-glucoside, myricetin, naringenin, and apigenin were detected in methanolic extract. Naringin (44.58 mg/g) was detected as a major identified phenolic compound in the extract of *C. paradisi* while pyrogallol (1.12 mg/g), cinnamic acid (0.95 mg/g), and caffeic acid (0.48 mg/g) were found as main identified phenolic acids. 0.88 mg/gm. of hesperidin was detected in methanol extract. While the addition of 14% dichloromethane to hot aqueous methanol extract gave the best yield of naringin (4.3%) as needle buff crystals with a melting point ≈ 165 ºC. H^1NMR spectroscopy of isolated naringin showed δ 12.05 (s, OH-4′), 9.61 (s, OH-5), 7.35 (d, *J* = 8.44 Hz, H-6'), 7.33 (d, *J* = 8.44 Hz, H-2'), 6.61 (d, *J* = 8.28 Hz, H-3', 5'), 6.12 (s, H-8), 6.09 (d, *J* = 2.2 Hz, H-6), 5.46 (dd, *J*=13.12, 2.28 Hz, H-2), 3.68 (H-3_{ax}), 2.72(H-3_{eq}), 5.15(Rha, H-1''), 5.30 (Glc, H-1'''), 1.16 (d, *J*= 6.84 Hz, Me-5'''). This H^1NMR data was in agreement with that of naringin [31, 32], which was eluted at the same R_t at 38.07 alongside co authentic naringin. While, acidifying methanolic extract of *C. paradisi* with 6% acetic acid (pH 3-4) led to the isolation of hesperidin (0.09%) as yellowish-brown crystals [33].H^1NMR spectrum of hesperidin showed a characteristic monomethoxylated flavanone 5.51(dd, *J*=11.92, 2.2Hz, H-2), 6.15 (s, H-6), 6.13 (s, H-8), 6.95 (d, *J*=6.76Hz, H-2′, 6′), 6.91 (d, *J*=8.6Hz, H-5′),3.81 (s, 3H, MeO-4′), 2.79 (dd, *J*= 17.4, 3.0Hz, 3ax), 5.00 (d, *J*=7.4Hz Glu-1″), 4.52 (s, Rh-1‴), 1.09 (d, *J*=6.08 Hz, Me-5‴) which was agreed with those published in the literature [32].

Concerning pectin, *Citrus paradisi* was used as a source of Pectin and its peel yielded 30.88 ± 1.68% of pectin as a white residue. The gel permeation chromatogram of isolated pectin (P2) revealed three major peaks with average molecular weights of 8.12×10^5, 4.16×10^4, and 7.80×10^3 g mol^{-1} with polydisperity of a polymer mixture 2.34, 1.027, and 1.088 respectively.

Fourier-transform infrared spectroscopy (FT-IR) is a consistent technique to ascertain the structural and physical properties of carbohydrates. The isolated pectin (P2) was scanned between wavenumber 4000 and 400 cm^{-1} which revealed the characteristic absorption bands of carbohydrate particularly pectin. The absorption bands at 3415.31 and 3190.65 cm^{-1} attributed to the hydroxyl group while the band at 2927.41 cm^{-1} attributed to the alkyl group. Meanwhile, the FT–IR spectrum data showed absorption bands at 1739.48 and 1644.02 cm^{-1} stretching modes of carbonyl groups assigned (mostly from esterified galacturonic acid, (C=O)ester) and carboxylate groups (COO^-), respectively [34]. The degree of esterification (% DM) was 29.32% which was calculated from FT -IR using equation [35].

$$\% DM = A_{1739}/ A_{1739}+ A_{1644}\times 100$$

Where A_{1739} is the area of the band at 1739 cm−1, and A_{1644}, that of the band at 1644 cm−1.

The band at 1405.85 cm^{-1} attributed to the symmetric stretch abilities of COO− and the stretch vibration of C-O within COOH. Whereas, the glycosidic linkage stretch vibration of C–O–C and C–O–H appeared at 1146.47 cm^{-1}. The isolated pectin was rich in uronic acids such as Gal A, which appeared as two intense bands at 1103.08 and 1018.23 cm^{-1} [36]. While, the absorption band at 1320.04 cm^{-1} was attributed to in-plane deformation modes of alcohol hydroxyl groups in the pyranose rings of the pectin chain, δ (C-O-H) pyranose [34]. The FT–IR spectrum did

not show a band around 1540–1560 cm^{-1}indicates that pectin did not bound to protein amide in the pectin molecules.

Concerned to antioxidant biomarkers; SOD, catalase and oxidative stress; MDA, a significant reduction in catalase and SOD activities concerned to 78.74 and 37.42 %, respectively, while, a markedly increasing in MDA level reached to 176.4%, in 100nm Ag–intoxicated mice. Severe reduction in 20 nm Ag reached to 65.96 and 42.52 %, respectively for catalase and SOD, but the elevation in MDA level recorded 200%. Treatment of both 20 and 100 nm particles with methanolic extract, pectin, hesperidin, and naringin exhibited ameliorations with different percentages, showed the highest of improvement with hesperidin followed by pectin, crude, and finally naringin.

3.2. Histology and histopathology analysis

Figure 1: Lung sections from Control (-ve control) showing normal alveoli with thin inter-alveolar septum, (A). +ve 20 nm showing alveoli with thick inter-alveolar septum. The septum is infiltrated by a large number of lymphocytes, type I and type II pneumocytes were also seen, ruptured alveoli (B). +ve 100nm showing congestion of pulmonary blood vessels, Lung of mice showing perivascular inflammatory cells infiltration focal pulmonary haemorrhage and perivascular massive inflammatory cells infiltration(C).

Figure 2: Lung of mice from control -ve given grapefruit showed no histopathological alterations with normal pulmonary alveoli. (A). -ve control given pectin shows normal pulmonary alveoli (B). +ve 20nm treated grape fruit showing almost normal alveoli with a thin inter-alveolar septum(C &D).+ve100 nm given grape fruit showing normal pulmonary alveoli with few focal pulmonary haemorrhages (E) +ve 100nm treated pectin revealed no histopathological alterations (F). Figure 3: Lung of mice from –ve control group given hesperidin showing normal pulmonary alveoli (A). –ve control treated with naringin showing no histopathological alterations (B) +ve20 nm given hesperidin, and naringin showing almost alveoli with thin inter-alveolar septum (C ,D). +ve 100 treated hesperidin showed nearly normal pulmonary alveoli with slight congestion of per alveolar blood capillaries (E). Positive group treated with 100 nm naringin, showing almost normal pulmonary alveoli (F) [H & E X 400].

4. Discussion

The systems of AgNP-incited cytotoxic reactions, responsive oxygen species (ROS) yield expanded apoptosis, DNA harm, and star aggravation [3]. Oxidative pressure as the main source of the unusual amassing of ROS can be responded to genuine cell harm, It plays a significant part in numerous kinds of cell injury, some of which can bring about DNA harm and apoptotic cell demise [4].

Nanoparticles can initiate the cell redox frameworks mostly in the lungs, where safe cells, including alveolar macrophages and neutrophils, go about as immediate ROS inducers [5].

The current results revealed a significant reduction in the nucleotide pools ATP, ADP, AMP, total adenylate level (TA), inorganic phosphate (IP), phosphate Potential (PP), and Adenylate Energy Charge (AEC) in 100 nm, Ag and an extensive reduction in 20 nm Ag particles, indicating the severe damage for the smallest particle sizes. These results are in contrast to the previous findings [17]. The significant diminution in the IP concentration in an intoxicated group, ATP reduction could be established as, when the body is ruled to metabolic pressure, a lot of phosphates are caught because of a strangely elevated level of phosphoryl acceptor [37].

AEC is a direct balance of the proportion of ATP fixation to add up to adenylate focus, which ranges in an incentive from 1 in the completely energized state to 0. Incomprehensibly, high estimations of AEC are routinely connected with high poison presentations, and reduced AEC esteems with low introduction. These inconsistencies might be explained by the failure of AEC estimations to satisfactorily assess cytosolic adenylate focuses, which are the basic boundaries in the regulation of enzymes [17].

Touchy pointers respected of anoxic conditions in lung tissues is a lessening in TA, AEC and the phosphate potential, the examination depicted in this investigation was directed to get biochemical proof to help the subsequent theory portrayed above, by deciding the adjustments in AEC, all-out adenine nucleotide focus and the groupings of debasement results of adenine nucleotide in the lung. After the introduction of Ag.

It could be pointed out that apoptosis is implicated in Ag–induced oxidative damage, one of important the different apoptotic pathways associated with the severity of respiratory chain damage, difficulty breathing with enlarged lungs size is the principally apoptotic roadway of mitochondrial which plays a great role in AgNP-induced cell deaths in the mitochondria as it considered as one of the

significant objective organelles for NP-actuated oxidative pressure [38].

Different metal oxide NP including Ag, Zn, Cu, Ti, and Si inspire ROS-interceded cell demise *via* dysfunction of mitochondria and hence affect electron transport chain, ATP formation, decrease in phosphate pool, phosphate potential (PP), AEC and TA levels [5].

The histopathological findings indicated the presence of alveoli with a thick inter-alveolar septum, a large number of lymphocytes, ruptured alveoli in 20 nm Ag, infiltrate the septum, while 100 nm show congestion of pulmonary blood vessels, perivascular inflammatory cell infiltration, focal pulmonary haemorrhage, and perivascular massive inflammatory cells.

The present results declared a significant reduction in vitamins C and E levels, as well as catalase and SOD activities were suppressed, while an obvious elevation in MDA levels was found in lung tissue. These reductions in antioxidant markers and elevations in oxidative stress may be due to, NP susceptibility inside the lung is deposited, causes mobilization of inflammatory phagocytes cells that create ROS and reactive nitrogen species (RNS), which in turn producing stimulating the cytokines either damaging or revolutionary to the cells of the lung [39]. The reduction in Vit. E (α-Tocopherol), in lung tissue, suggested the presence of inflammation associated with oxidative damage as vitamin E is accounted for to act about as a striking calming and cancer prevention agent for protection against degenerative cycles initiated by oxidative pressure [40]. The decrease in Vit. C in lung tissue conjectures the oxidative adjustment of LDL's, which adds to the atherosclerotic cycle for their cytotoxic impacts, incitement of extremist scroungers receptors and their effect on the motility of monocytes and macrophages [41].

A fundamentally expanded level of MDA, besides, a reduction in antioxidant enzymes in lung tissues post-induction of 20 and 100 nm Ag compared to control group [42]. The SOD, GPx, and catalase enzymes assume a huge function in the balance of ROS and forestall the proliferation of oxidative pressure interceded harm [43]. In this investigation, the movement of SOD and catalase were diminished by the organization of Ag, expanding the degree of free revolutionaries in the cell, trailed by peroxidation of the film lipids, which prompts precariousness and, eventually, breakdown of the cell. Lysosomal protein delivering or really the creation of ROS brought about by Ag would incite mitochondria-intervened apoptosis [40]. Nanoparticle size is a significant trademark basic statement and destiny in the lung, smaller nanoparticles may cross cell boundaries all the more effectively by balancing explicit take-up and endocytic measures [44]. The expanded bio-accessibility joined with a bigger surface zone may potentiate connection with cell organelles, expanding responsive oxygen species creation, aggravation, and cytotoxicity [45].

Molecule size assumes a significant function in the take-up energy of NPs in the cells, it was discovered that the Ag was prevalently collected in the lungs, spleen, liver, and kidneys of rodents dosed with AgNPs, recommending the AgNPs moved and gathered into explicit objective organs where they may additionally produce Ag [46]. The vascular injury could be instigated by the rehashed pneumonic presentation of AgNPs (20 nm). In any case, high groupings of AgNP in the circulatory framework may cause serious toxicities [47]. Lymphocyte and macrophage penetration were uncovered as the key perceptions for AgNP prompted morphological changes in lung tissue with cell degeneration, recovery, and necrosis [46]. Nanoparticles cause inflammation and safe reaction while associating with the tissues, which is additionally a key component of Nanotoxicity. In this way, the gentle disturbance seen in the lung was proposed to be related with the recognition process of the immune system [48] The dissolved Ag+ contributed to most of the toxic effects caused by AgNP, The conceivable system of AgNP-induced genotoxicity was engaged with the interference of ATP combination, after the interruption of the mitochondrial respiratory chain and overabundance creation of serum responsive oxygen species (ROS) [49]. Ag particles are associated with tissue disturbance and that these particles are delivered from Ag-NP assembled by alveolar macrophages. This cycle seems to harm alveolar macrophages after some time, as proposed by the various swollen macrophages saw in the Ag50-PVP NP-loaded lung parenchyma following three weeks [4].

Interestingly, oral administration of *C. paradisi* peels methanolic extract, naringin, hesperidin, and pectin to Ag-NP intoxicated mice led to ameliorate ATP, ADP, AMP, TA, IP, PP, AEC, vitamin E and C levels, SOD, and catalase antioxidant enzymes in lung tissue along with the improved architecture of lung tissue. The flavonoids could be attributed to anti-inflammatory and antioxidant properties in lung disease [50]. The total antioxidant capacity of Citrus fruit is depending on their phytochemical composition and content of antioxidants that may act as a protection against the aggregation of ROS/RNS as well as act as both preventatives and chain scission factors that efficiently damaging

the reactive oxygen species [51]. Naringin that was identified as the main flavonoid in *C. paradisi* peel, exhibits effective protection against AgNPs induced lung injury Moreover, naringin reduced up-regulation of MMP-9 and its inhibitor TIMP-1, aspiratory malonaldehyde, and hydroxyproline just as pneumonic fibrosis. These highlights were related to expanded superoxide dismutase, glutathione peroxidase (GSH-Px), and heme oxygenase (HO-1) exercises [50]. Also, naringin exhibited strong antioxidant activity which improved antioxidant enzymes (SOD) and catalase, reduced the lipid peroxidation product and hydroperoxides in isoproterenol-induced Wistar rats, as well as NAD (PH) [52].

While hesperidin, decreased the inflammatory mediators and enhanced the anti-inflammatory cytokines by its immunomodulatory effect in bronchoalveolar lavage fluid (BALF) in murine [53]. Whereas, pre-administration of hesperidin applies a defensive impact against lung harm initiated by intestinal I/R injury in rodents by significantly decreasing the neutrophils accumulation, MPO, MDA levels as well as reducing the activity of glutathione. Also, it can repress both the arrival of free revolutionaries from neutrophils and oxidative harm to the cellular membrane [54].

The antioxidant effect of phenolic acid showed various degrees of scavenging activity of free radicals depending on the dehydrogenation capacity of the hydroxyl group and the influence of ortho substitution on the benzene ring [51]. Among phenolic acids, *p*-coumaric acid that is identified in the methanolic extract, plays a key role in cellular defence due to its antioxidant and anti-inflammatory effects. It can convert to other phenolic acids such as chlorogenic acid, flavonoids, and other secondary metabolites [55]. Furthermore, chlorogenic acid that also identified in the methanolic extract, has anti-inflammatory and antioxidant diagnostics that suppress the production of pro-inflammatory cytokines and have ensured against aggravation and tissue injury in rheumatoid joint pain, hepatitis and colitis. Moreover, it stifled the seriousness of incendiary penetrate and alveolar thickness followed by the decrease of invaded insusceptible cells, for example, neutrophil into alveoli [56].

On the other hand, various pharmacological studies have shown the bioactivity of pectin, including immunoregulatory, anti-inflammatory, hypoglycemic, antibacterial, antioxidant, and antitumor activities [57]. Similarly, it can straightforwardly actuate the safe capacity of macrophages and advance the creation of cytokines**.** As a negatively charged compound, pectin plays a major role in the detoxification of heavy metals because of its high capability in binding heavy metals [57]. Alike, it enhances endogenous antioxidant enzymes and the disposal of free radicals due to its antioxidant property [51].

Conclusions

In conclusion, this research reveals insight into the underlying toxic effects of AgNPs which is confirmed by modifications in some cell biochemical boundaries, genotoxicity, mutagenicity, and histopathological records on Albino Swiss mice. Methanol, pink grapefruit extract, hesperidin, naringin, pectin can enhance the harmfulness initiated by means of AgNPs and record a perceptible level of progress in the chose biomarkers. So, a possible explanation for the therapeutic target's records in the current study could be attributed to the bioactive secondary metabolites in the grapefruit as a methanolic extract, hesperidin, naringin besides pectin, owing to their strong antioxidant, anti-inflammatory and free radical scavenging properties.

Authors' Contributions

EAY conducted the experiments**,** Formal analysis and Data curation.

HFA, AAM and SAA Writing the manuscript, review and editing. All authors approved the final version of the published manuscript

Declaration of Conflicting Interests

The authors declare that there are no conflicts of interest with respect to the research.

Funding

This research received no specific grant from any funding agency

References

[1] Ali SA, Arafa AF, Aly HF, Ibrahim NA, Kadry MO, Abdel-Megeed RM, Hamed MA, Farghal AA, El Regal NS, Fouad GI, Khalil WKB, Refaat EA. DNA damage and genetic aberration induced via different sized silver nanoparticles: Therapeutic approaches of Casimiroa edulis and Glycosmis pentaphylla leaves extracts. J Food Biochem 2020; e13398: 1-14

[2] Weldon BA, Faustman E, Oberdörster G, Workman T, Griffith WC, Kneuer C, Yu I J. Occupational exposure limit for silver nanoparticles: Considerations on the derivation of a general health-based value. Nanotoxicology 2016; 10: 945–956.

[3] Bin-Hsu Mao, Zi-Yu Chen, Ying-Jang Wang, Shian-Jang Yan. Silver nanoparticles have lethal and sublethal adverse effects on development and longevity by inducing ROS-mediated stress responses Scientific Reports 2018; 8: 2445-2452

[4] Wiemann M, Vennemann A, Blaske F, Sperling M, Karst U. Silver Nanoparticles in the Lung: Toxic Effects and Focal Accumulation of Silver in Remote Organs. Nanomaterials. 2017; (7) 441: 1-26

[5] Manke A, Wang L, Yon Rojanasakul Y. Mechanisms of Nanoparticle-Induced Oxidative Stress and Toxicity. BioMed Research International 2013; 1-15

[6] Stensberg MC, Wei Q, McLamore ES, Porterfield DM, Wei A, Sepúlveda MS. Toxicological studies on silver nanoparticles: Challenges and opportunities in assessment, monitoring and imaging. Nanomedicine 2011; 6: 879–898

[7] Fewtrell L, Majuru B, Hunter PR. A re-assessment of the safety of silver in household water treatment: Rapid systematic review of mammalian in vivo genotoxicity studies. Environ. Health Glob Access Sci. Source 2017; 16: 66

[8] Guo H, Zhang, J, Boudreau M, Meng J, Yin J, Liu J, Xu H. Intravenous administration of silver nanoparticles causes organ toxicity through intracellular ROS-related loss of inter-endothelial junction. Part. Fibre Toxicol 2016; 13: 21

[9] Chen Q, Wang D, Tan C, Hu Y, Sundararajan B, Zhou Z. Profiling of Flavonoid and Antioxidant Activity of Fruit Tissues from 27 Chinese Local Citrus Cultivars. Plants (Basel) 2020; 5, 9(2): 196

[10] *Oueslati A, Salhi-Hannachi A, Luro Fr, Vignes H, Mournet P, Ollitrault, P.* "Genotyping by sequencing reveals the interspecific C. maxima / C. reticulata admixture along the genomes of modern citrus varieties of mandarins, tangors, tangelos, organelles and grapefruits". *PLOS ONE 2017; 12 (10): e0185618*

[11] Ahmed S, Rattanpal HS, Gul K, Dar RA, Sharma A. Chemical composition, antioxidant activity, and GC-MS analysis of juice and peel oil of grapefruit varieties cultivated in India. Journal of Integrative Agriculture 2019; 18 (7): 1634–1642

[12] Cristóbal-Luna JM, Álvarez-González I, Madrigal-Bujaidar, E., Cevallos GC Grapefruit and its biomedical, antigenotoxic and chemopreventive properties. Food Chem. Toxicol. 2018; 112: 224–234

[13] Zheng H, Zhang Q, Quan J, Zheng Q, Xi W. Determination of sugars, organic acids, aroma components, and carotenoids in grapefruit pulps. Food Chemistry 2016; 205:112–121

[14] Deng W, Liu K, Cao S, Sun J, Zhong B, Chun J. Chemical Composition, Antimicrobial, Antioxidant, and Antiproliferative Properties of Grapefruit Essential Oil Prepared by Molecular Distillation. Molecules 2020; 25 (1): 217.

[15] Minzanova ST, Mironov VF, Arkhipova DM. et al. Biological Activity and Pharmacological Application of Pectic Polysaccharides: A Review. Polymers (Basel). 2018; 10 (12):1407

[16] Zilic S, Serpen A, Akillioglu G, Jankovic M, Gokmen V. Distributions of phenolic compounds, yellow pigments and oxidative enzymes in wheat grains and their relation to antioxidant capacity of bran and debranned flour. Journal of Cereal Science 2012; 56: 652-658

[17] Ali SA, Aly HF, Faddah LM, Zaidi ZF. Dietary supplementation of some antioxidants against hypoxia. World J Gastroenterol. 2012; 28, 18(44): 6379–6386

[18] Lamprecht W, Trauschold I. Determination of adenosine-5-triphosphate with hexokinase and glucose-6-phosphate dehydrogenase. In: Bergmeyer HU, editor. Methods of enzymatic analysis. London: Verlage Chemie Wein Heim Academic Press 1974; 2101–2109

[19] Jaworek D, Gruber W, Bergmeyer HU. Adenosine-5-diphosphate and adenosine-5-monophosphate. In: Bergmeyer. Methods of enzymatic analysis. London: Verlage Chemie Wein Heim Academic Press: 1974; 2126–2131

[20] Van Waarde A, Van den Thillart G, Erkelens C, Addink A, Lugtenburg J Functional coupling of glycolysis and phosphocreatine utilization in anoxic fish muscle. An in vivo 31P NMR study. J Biol Chem 1990; 265:914–923.

[21] Fiske CH, Subbarow Y. The colorimetric determination of phosphorous. J. Biol.Chem 1925; 66: 375-400.

[22] Buege JA., Aust SD. Microsomal lipid, Peroxidation. In: Flesicher S, Packer L (Eds.), Methods in Enzymology. Academic Press, New York 1978; 52: 302–310

[23] Aebi H. Catalase in vitro Methods Enzymol 1984; 105:121-126

[24] Nishikimi M, Rae N A, Yagi K. The occurrence of superoxide anion in the action reduced phenazine methosulphate and molecular oxygen. Biochem. Biophys. Res. Commun 1972; 46:849-853

[25] Robitaille L, Hoffer LJ. A simple method for plasma total vitamin C analysis suitable for routine clinical laboratory use. Nutr J 2016; 15: 40

[26] Das KK, Jargar JG, Hattiwale SH, Yendigeri SM, Das S, Dhundasi SA. Serum vitamin E (α-tocopherol) estimation: a potential biomarker of antioxidant status evaluation on heavy metal toxicities. Curr Biomark 2013; 3: 36-43.

[27] Abo Zaid OAR, El-Batal AI, Effat S. Biochemical Evaluation of Antitumor Activity of Irradiated Citrus Pectin: oxidants and antioxidants content. International Journal of Pharma Sciences 2018; 8 (4): 1960-1964

[28] Li W, Kandhare AD, Mukherjee AA, Bodhankar SL. Hesperidin, a plant flavonoid accelerated the cutaneous wound healing in stereptozotocin-induced Diabetic rats: role of TGF-B/SMADS and ANG-1/TIE-2 Signaling pathways. EXCLI Journal 2018; 17: 399-419

[29] Kumar SR, Ramli ESM, Abdul Nasir NA, Ismail NHM, Fahami NM. Preventive Effect of Naringin on Metabolic Syndrome and Its Mechanism of Action: A Systematic Review Evidence-Based Complementary and Alternative Medicine 2019; 1-11

[30] Hirsch C, Zouain CS, Alves JB, Goes A. Induction of protective immunity and modulation of granulomatous hypersensitivity in mice using PIII, an anionic fraction of Schistosoma mansoni adult worm. Parasitology 1997; 115: 21–28

[31] Maltese F, Erkelens C, van der Kooy F, Choi YH, Verpoorte R. Identification of natural epimeric flavanone glycosides by NMR spectroscopy. Food Chemistry 2013; 116: 575-579

[32] Tang K S C, Konczak I, Zhao J. Identification and quantification of phenolics in Australian native mint (Mentha australis R. Br.) Food Chemistry 2016; 192: 698–705

[33] Sharma P, Pandey P, Gupta R, Roshan1 S, Garg A, Shulka A, Pasi A. Isolation and characterization of hesperidin from orange peel. Journal of Pharm Research 2013; 3(4): 3892-3897

[34] Ciriminna R, Fidalgo A, Delisi R, Tamburino A, Carnaroglio D, Cravott G, Ilharco LM, Pagliaro M. Controlling the Degree of Esterification of Citrus Pectin for Demanding Applications by Selection of the Source. ACS Omega 2017; 2: 7991−7995.

[35] Kyomugasho C, Christiaens S, Shpigelman A, Van Loey AM, Hendrickx ME. FT-IR spectroscopy, a reliable method for routine analysis of the degree of methyl esterification of pectin in different fruit- and vegetable-based matric. Food Chemistry 2015; (1)176: 82-90

[36] La Cava EL, Gerbino E, Sgroppo S C, Gómez-Zavaglia A. Characterization of Pectins Extracted from Different Varieties of Pink/Red and White Grapefruits [Citrus Paradisi (Macf.)] by Thermal Treatment and Thermo sonication. Journal of Food Science 2018; 83(6): 1613–1621.

[37] Overton JD, Adams GS, McCall RD, Kinsey ST. High-energy phosphate concentrations and AMPK phosphorylation in skeletal muscle from mice with inherited differences in hypoxic exercise tolerance. Comp Biochem Physiol A MolIntegr Physiol 2009; 152:478–485

[38] Gomes A, Sengupta J, Datta P, Ghosh S, Gomes A. Physiological Interactions of Nanoparticles in Energy Metabolism, Immune Function and Their Biosafety: A Review. Journal of Nanoscience and Nanotechnology 2016; 16: 92–116

[39] Li JJ, Muralikrishnan S, Ng CT, Yung LY, Bay BH. Nanoparticle-induced pulmonary toxicity. *Experimental Biology and Medicine*. 2010; 235(9): 1025–1033

[40] Moradi A, Nasrin Ziamajidi N, Ghafourikhosroshahi A, Abbasalipourkabir, R. Effects of vitamin A and vitamin E on attenuation of titanium dioxide nanoparticles-induced toxicity in the liver of male Wistar rats Molecular Biology Reports 2019; 46: 2919–2932

[41] Sun Q, Tan D, Ze Y, Sang X, Liu X, Gui S. Pulmotoxicological effects caused by long-term titanium dioxide nanoparticles exposure in mice. J Hazard Mater 2012; 235: 47–53

[42] Meena R, Paulraj R. Oxidative stress mediated cytotoxicity of TiO2 nanoanatase in liver and kidney of Wistar rat. Toxicol Environ Chem 2012; 94(1): 146–163

[43] Ighodaro O, Akinloye O. First line defense antioxidants-superoxide dismutase (SOD), catalase (CAT), and glutathione peroxidase (GPX): their fundamental role in the entire antioxidant defense grid. Alex J Med 2017; 54:287–293

[44] Seiffert J, Hussain F, Wiegman C, Li F, Bey L, Baker W, et al. Pulmonary Toxicity of Instilled Silver Nanoparticles: Influence of Size, Coating and Rat Strain. PLoS ONE 2015; 10(3): e0119726

[45] Carlson C, Hussain SM, Schrand AM, Braydich-Stolle LK, Hess KL, Jones RL. Unique cellular interaction of silver nanoparticles: size-dependent generation of reactive oxygen species. The journal of physical chemistry B. 2008; 112(43): 13608–19

[46] Wen H, Dan M, Yang Y, Lyu J, Shao A, Cheng X, Chen L, Xu L. Acute toxicity and genotoxicity of silver nanoparticle in rats. PLOS ONE 2017; 27: 1-16.

[47] Tiwari DK, Jin T, Behari J. Dose-dependent in-vivo toxicity assessment of silver nanoparticle in Wistar rats. Toxicology mechanisms and methods 2011; 21(1): 13–24.

[48] Katsumiti A, Gilliland D, Arostegui I, Cajaraville MP. Mechanisms of Toxicity of Ag Nanoparticles in Comparison to Bulk and Ionic Ag on Mussel Hemocytes and Gill Cells. PloS one 2015; 10(6): e0129039

[49] Thannickal VJ, Fanburg BL. Reactive oxygen species in cell signaling. Am J Physiol-Lung Cell Mol Physiol 2000; 279 (6): L1005-L1028

[50] Lago J, Toledo-Arruda, A, Mernak M, Barrosa K, Martins, M, Tibério I, Prado C. Structure-Activity Association of Flavonoids in Lung Diseases. Molecules, 2014; 19 (3): 3570–3595

[51] Zou Z, Xi W, Hu Y, Nie C, Zhou Z. Antioxidant activity of Citrus fruits. Food Chemistry, 2016; 196: 885–896

[52] Alam MA, Subhan N, Rahman MM, Uddin SJ, Reza HM, Sarker S D. Effect of citrus flavonoids, naringin and naringenin, on metabolic syndrome and their mechanisms of action. Adv Nutr 2014; 5(4): 404-417

[53] Wei D, Ci X, Chu X, Wei M, Hua S, Deng X. Hesperidin suppresses ovalbumin-induced airway inflammation in a mouse allergic asthma model. Inflammation 2012; 35:114–121

[54] Bayomy NA, Elshafey SH, ElBakary R H, Abdelaziz EZ. Protective effect of hesperidin against lung injury induced by intestinal ischemia/reperfusion in adult albino rats: Histological, immunohistochemical, and biochemical study. Tissue and Cell 2014; 46(5): 304–310

[55] Kheiry M, Dianat M, Badavi M, Mard SA, Bayati V. P-Coumaric acid protects cardiac function against lipopolysaccharide-induced acute lung injury by attenuation of oxidative stress. Iran J Basic Med Sci 2019; 22 (8):949-955

[56] Ohkawara T, Takeda H, Nishihira J. Protective effect of chlorogenic acid on the inflammatory damage of pancreas and lung in mice with l - arginine-induced pancreatitis. Life Sciences 2017; 190: 91–96

[57] Mehrandish R, Rahimian A, Shahriary A. Heavy metals detoxification: A review of herbal compounds for chelation therapy in heavy metals toxicity. J Herbmed Pharmacol 2019; 8(2): 69-77.

.

Table (1): Effect of grape extract and active compounds of pectin, hesperidin .and naringin on ATP, ADP, AMP, TA, IP443 AEC and PP in lung of mice control mice

	Normal control treated				
Parameters	Normal control	Grape	pectin	Hesp.	Narin.
ATP	0.068 ±0.002^{a}	0.062 ±0.003^{a}	0.064 ±0.001^{a}	0.065 ±0.001^{a}	0.066 ±0.001^{a}
ADP	0.028 ±0.001^{b}	0.021 ±0.001^{c}	0.025 ±0.005^{c}	0.022 ±0.005^{c}	0.023 ±0.005^{c}
AMP	0.013 ±0.003^{e}	0.012 ±0.001^{e}	0.010 ±0.002^{e}	0.011 ±0.002^{e}	0.010 ±0.002^{e}
TA	0.109± 0.002^{a}	0.095±0.003 ^{a}	0.099± 0.001^{a}	0.098± 0.001^{a}	0.099± 0.001^{a}
IP	0.59 ±0.071^{a}	0.57 ±0.017^{ab}	0.48 ±0.022^{ab}	0.47 ±0.022^{ab}	0.46 ±0.022^{ab}
AEC	0.79 ±0.024^{d}	0.76 ±0.022^{d}	0.75 ±0.015^{d}	0.77 ±0.013^{d}	0.74 ±0.014^{d}
PP	5.14 ±0.82^{b}	5.30 ±0.42^{b}	4.82 ±0.62^{b}	4.88 ±0.62^{b}	4.80 ±0.62^{b}

Data represents means ± SD of 15 mice in every group, data are expressed as µmoles /g. wet weight for ATP, ADP, AMP and TA while IP, AEC and PP are without dimension

Table (2): Effect of grape extract and active compounds of pectin, hesperidin .and naringin on ATP, ADP, AMP, TA, IP,AEC and PP in lung of mice post oral Exposure to 20nm and 100nm Ag

	Ag 20nm treated					Ag100nm treated				
Parameters	Ag 20	Grape	pectin	Hesp.	Narin.	Ag 100	Grape	pectin	Hesp.	Narin.
ATP	0.020±0.017^{b}	0.046±0.005^{c}	0.048 ±0.009^{c}	0.051 ±0.031^{c}	0.041±0.042^{c}	0.022±0.017^{b}	0.056±0.005^{c}	0.058±0.009^{c}	0.061±0.042^{a}	0.055±0.031^{c}
ADP	0.011±0.001^{d}	0.018±0.002^{e}	0.019 ±0.001^{e}	0.020 ±0.003^{c}	0.017±0.003^{e}	0.014±0.001^{d}	0.021±0.003^{c}	0.022±0.002^{c}	0.024±0.003^{c}	0.018±0.001^{d}
AMP	0.004±0.001^{f}	0.012±0.004^{c}	0.014 ±0.002^{a}	0.017 ±0.001^{a}	0.011±0.008^{c}	0.006±0.001^{f}	0.015±0.008^{b}	0.015±0.008^{b}	0.016±0.001^{a}	0.014±0.004^{b}
TA	0.042±0.001^{f}	0.092±0.008^{a}	0.095± 0.009^{a}	0.101± .001^{a}	0.087±0.031^{c}	0.035±0.001^{f}	0.076±0.008^{c}	0.081±0.009^{c}	0.088±0.001^{c}	0.069±0.031^{d}
IP	0.99±0.033^{d}	0.55±0.038^{ab}	0.51 ±0.047^{ab}	0.49 0.068^{ab}	0.57±0.068^{ab}	0.87±0.033^{b}	0.36±0.038^{c}	0.33±0.01^{c}	0.31±0.047^{c}	0.40±0.068^{c}
AEC	0.52±0.019^{f}	0.72±0.004^{d}	0.73 ±0.026^{d}	0.73 ±0.026^{d}	0.70±0.005^{d}	0.45±0.019^{f}	0.62±0.026^{c}	0.66±0.005^{c}	0.69±0.026^{c}	0.61±0.015^{c}
PP	0.65±0.43^{d}	4.60±0.44^{b}	5.10 ±0.34^{b}	5.70 ±0.41^{b}	4.40±0.68^{b}	0.85±0.43^{d}	3.50±0.44^{c}	3.70±0.41^{c}	4.10±0.34^{b}	3.40±0.68^{c}

Data represents means ± SD of 15 mice in every group, data are expressed as µmoles /g. wet weight for ATP, ADP, AMPand TA while IP,AEC and PP are without dimension

Table (3): Effect of grape extract and active compounds ofpectin, Hesp.andNarin.onantioxidant enzymes,catalase, SOD enzyme activities, oxidative stress biomarker ;MDA , Vit C and Vit E in lung of control mice

	Normal control treated				
Parameters	Normal control	Grape	pectin	Hesp.	Narin.
Catalase	15.66 ±0.071^{a}	14.85 ±0.017^{a}	14.55 ±0.022^{a}	13.77 ±0.022^{a}	13.66 ±0.022^{a}
SOD	317.5 ±0.024^{a}	289.9 ±0.022^{b}	295.1 ±0.015^{b}	305.5 ±0.013^{d}	299.9 ±0.014^{b}
MDA	353 ±0.82^{a}	435 ±0.42^{b}	471 ±0.62^{b}	494 ±0.62^{b}	482 ±0.62^{b}
Vit.C	20.35 ±1.05^{a}	19.57 ±0.017^{a}	19.48 ±0.022^{a}	18.47 ±0.022^{a}	20.46 ±0.022^{a}
Vit. E	40.12 ±1.05^{a}	38.22 ±0.022^{a}	39.85 ±0.015^{a}	38.87 ±0.013^{a}	37.84 ±0.014^{a}

Data represents means ± SD of 15 mice in every group. Catalase enzyme, are expressed as unit/g tissue SOD as μmol/mg protein for, MDA are expressed as µg/mg protein ,Vit.C, Vit. E are expressed as Unit/m. Statistical analysis is carried out using SPSS computer program (version,8) coupled with Co-Stat computer program , where unshared letters between groups are the significance value at $P \leq 0.5$.

Table (4): Effect of grape extract and active compounds of *Pectin* , Hesp. and Narin. on antioxidant enzymes ; catalase , SOD enzyme activities and oxidative stress biomarker ;MDA in lung of mice post oral exposure to20nm and 100nm Ag

Parameters	Ag 20nm treated					Ag 100nm treated				
	Ag 20nm	Grape	pectin	Hesp.	Narin.	Ag 100nm	grape	pectin	Hesp.	Narin.
Catalase	5.33±0.03^{f}	9.50±0.047^{e}	10.50±0.038^{c}	11.20±0.01^{c}	8.00±0.068^{e}	3.33±0.033^{f}	10.0±0.047^{e}	11.20±0.038^{c}	12.4±0.01^{c}	7.5±0.07^{e}
SOD	182.5±0.02^{f}	229.9±0.015^{c}	231.1±0.04^{c}	250.0±0.026^{c}	217.5±0.005^{c}	198.7±0.019^{f}	245.0±0.026^{e}	283.1±0.005^{b}	290.0±0.004^{b}	238.7±0.02^{e}
MDA	1059±0.43^{f}	647±0.68^{c}	576±0.41^{c}	506±0.44^{c}	706±0.34^{e}	976.0±0.43^{f}	647±0.34^{c}	611±0.44^{c}	576±0.68^{b}	647±0.41^{c}
Vit.C	10.21±0.033^{b}	15.33±0.01^{c}	16.0±0.047^{c}	16.36±0.038^{c}	15.0±0.068^{c}	11.87±0.033^{b}	16.31±0.047^{c}	16.33±0.01^{c}	17.56±0.038^{c}	15.4± 0.068^{c}
Vit. E	20.0±0.019^{f}	31.73±0.005^{c}	32.66±0.004^{c}	33.70±0.026^{c}	29.9±0.015^{c}	22.4±0.019^{f}	33.78±0.005^{c}	34.79±0.004^{c}	35.7±0.026^{c}	31.7±0.015^{c}

Data represents means ± SD of 15 mice in every group. Catalase enzyme, are expressed as unit/g tissue SOD as μmol/mg protein for, MDA are expressed as µg/mg protein , Vit.C, Vit. E are expressed as Unit/m. Statistical analysis is carried out using SPSS computer program (version,8) coupled with Co-Stat computer program , where unshared letters between groups are the significance value at $P \leq 0.5$.

Table (5): Histopathological lung lesions score in mice post oral exposure to 20nm and 100nm Ag and after treatment of bioactive compounds

Histopathological lesion	Ag 20nm treated					Ag 100nm treated				
	Ag 20nm	Grape	pectin	hesperidin	naringin	Ag 100 nm	grape	pectin	hesperidin	naringin
congestion of pulmonary blood vessels	+++	+	+	-	-	+++	+	++	++	-
perivascular inflammatory cells infiltration	+++	-	-	-	-	+++	++	++/-	-	-
focal pulmonary hemorrhage	++	+	+	+	+	+++	++	-	-	-

(-) no change (+) mild change (++) moderate change (+++) severe change

Table (6): Qualification and quantification of some phenolic compounds identified in *Citrus paradisi* methanolic extract using HPLC/DAD analysis

Compound	R_t	λ_{max} /nm	Concentration (mg/g)
			Methanol crude extract
Pyrogallol	4.72	280	1.12
p-Hydroxybenzoic acid	14.94	280	0.07
Chlorogenic acid	20.73	320	0.11
Caffeic acid	21.49	320	0.48
Ferulic acid	31.93	320	0.04
p-Coumaric acid	37.01	280	0.03
Narirutin	37.37	280	1.80
Naringin	38.07	280	44.58
Hesperidin`	38.69	280	0.88
Apigenin-7-glucoside	38.70	320	1.17
Myricetin	39.47	360	0.10
Cinnamic acid	42.88	280	0.95
Naringenin	45.01	280	0.03
Apigenin	46.35	320	0.02

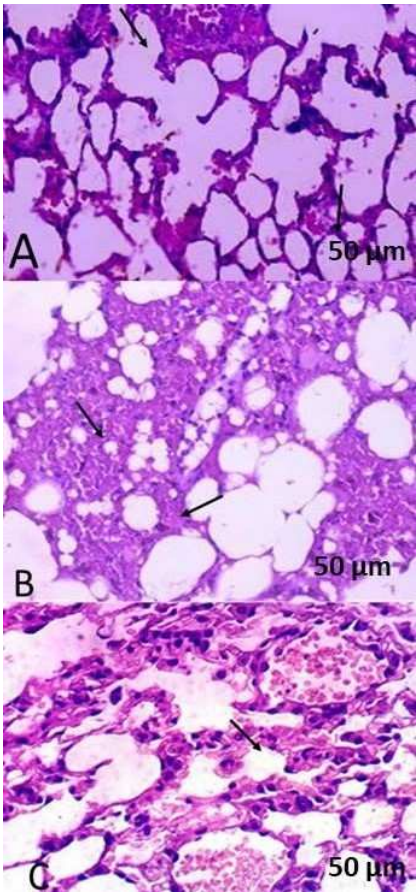

Figure 1: (A) Lung sections from Control showing normal alveoli. **(B)**20nm showing alveoli with thick inter-alveolar septum, **(C)** 100nm showing congestion of pulmonary blood vessels with perivascular inflammatory cells infiltration focal pulmonary hemorrhage (scale bar: 50 µm) [HE:x 400]

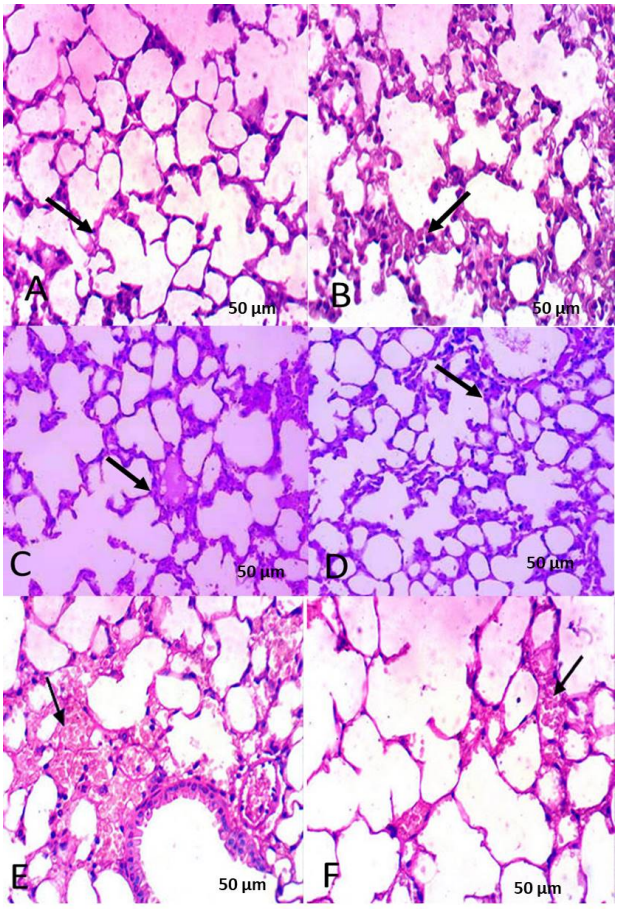

Figure2: (A) Lung of control given grapefruit **(B)** control given pectin showing normal pulmonary alveoli. **(C)** 20nm treated grape fruit. **(D)** 20nm treated pectin **(E)**100nm given grape fruit.**(F)** 100nm treated pectin (scale bar: 50 µm)[HE:x 400]

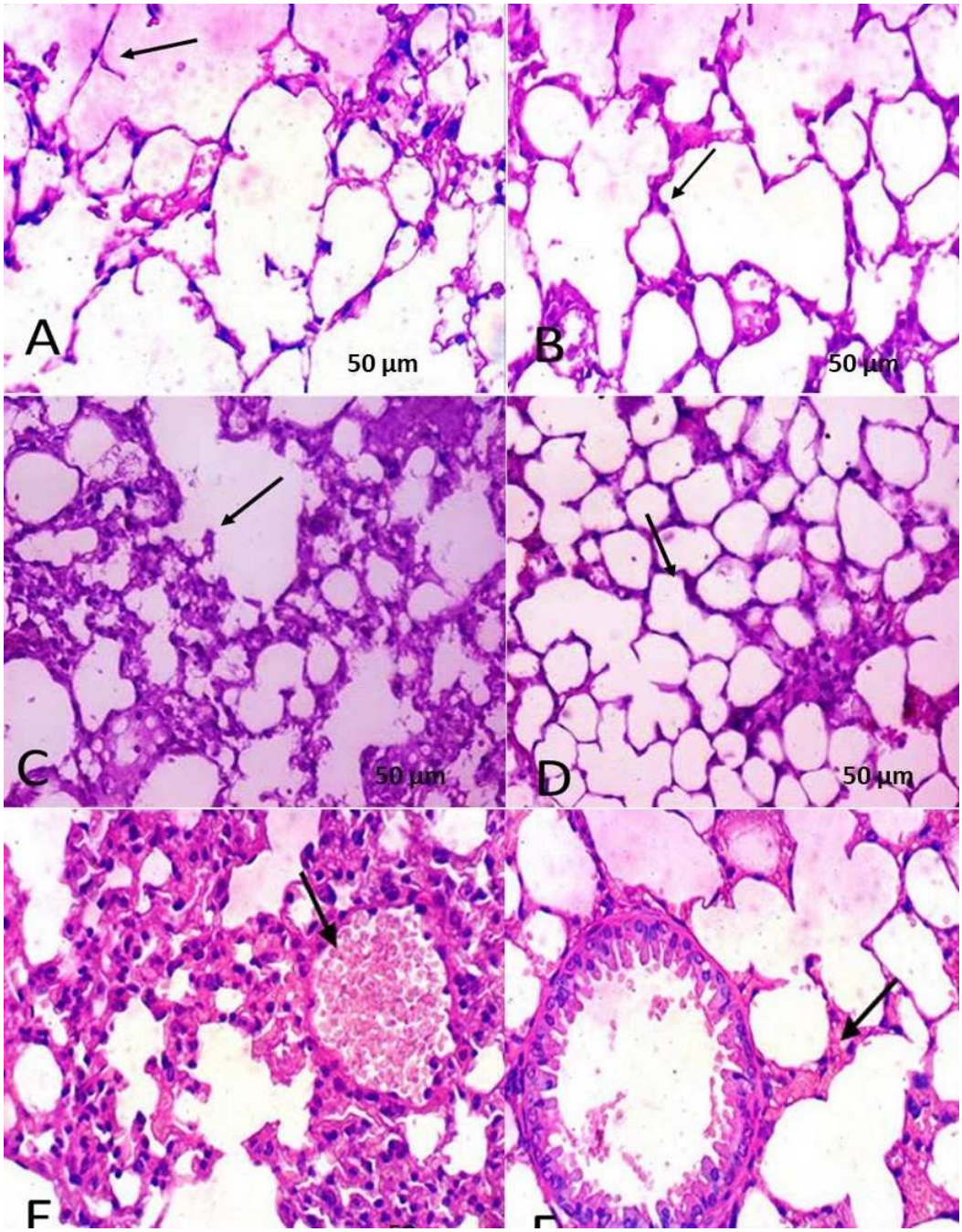

Figure 3: (A) Lung of control given hesperidin. **(B)**Control treated with naringin. **(C&D)**20nm given hesperidin and naringin respectively. **(E)** 100 nm, treated hesperidin. **(F)**100nm given naringin showing almost normal pulmonary alveoli (scale bar: 50 µm)[HE: x 400]